Mol. Cells *31*, 17-23, January 31, 2011
DOI/10.1007/s10059-011-0003-0

Molecules and Cells

Analysis of Gene Expression Profiles of Liver Stellate Cells During Liver Regeneration in Rats

Xu Cunshuan[1,2,*], Chen Xiaoguang[2,3], Chang Cuifang[2,3], Wang Gaiping[1,2], Wang Wenbo[1,2], Zhang Lianxing[1,2], Zhu Qiushi[1,2], Wang Lei[1,2], and Zhang Fuchun[3]

This study performed a large-scale, high-throughput analysis of transcriptional profiling of liver stellate cells (LSCs) at the cellular level to investigate changes in the biological activity of LSCs during rat liver regeneration (LR) and the relation of these changes to LR. First, a rat liver regeneration model was established by partial hepatectomy (PH). Stellate cells were isolated in high purity and yield from the regenerating rat liver by Percoll density gradient centrifugation and immunomagnetic bead sorting. The changes in gene expression of LSCs after PH were examined using a rat genome 230 2.0 array composed of 24622 genes. The results indicated that 10241 of the 24622 genes investigated on the array were differentially expressed in LSCs. Of the 10241 genes, 1563 known genes were related to LR, which were grouped into three major gene expression clusters according to three-fold cut-off threshold: the up-regulated gene cluster, the down-regulated gene cluster, and the cluster composed of genes showing complex changes in expression. Additionally, the genes were grouped into those involved in transcription regulation, signal transduction, transport, cellular metabolism, inflammation and immunity by functional analysis. When gene expression profiles were combined with the results of gene functional analysis, most of the genes involved in cytokine secretion and retinol metabolism in LSCs were significantly enriched in the cluster characterized by decreased expression, whereas genes involved in lipid metabolism were mostly enriched in the cluster showing increased expression. Based on further analysis of genes expressed in a phase-dependent manner during LR, it was suggested that lipid metabolism in LSCs was enhanced in the whole regeneration process, and that immune response and cytokine secretion were impaired during all three regenerative phases.

INTRODUCTION

Liver stellate cells (LSCs) are a population of specific mesenchymal cells in the liver (Zheng et al., 2009). The quiescent LSCs are usually located in the space of Disse, making up approximately one-third of nonparenchymal cells and 8-13% of total liver cells (Mohammed and Khokha, 2005). LSCs have a spindle-shaped cell body with round or oval shaped nuclei, and contain retinol and lipid-storing droplets of different sizes (Atzori et al., 2009). Under normal conditions, LSCs possess a high capacity to store vitamin A (Budny et al., 2007), and also serve as antigen presenting cells to regulate immunity and inflammation (Friedman, 2008). After liver injury, LSCs are activated and pass from the quiescent state to the proliferative state during which they acquire the myofibroblast phenotype (Passino et al., 2007). This transition is companied by the loss of droplets and the secretion of a large amount of extracellular matrix components, such as the adhesion molecules ICAM1, VCAM1, NCAM, which are involved in recruiting inflammatory cells (Kubota et al., 2007).

Although there is some evidence supporting the involvement of LSCs in liver regeneration (LR), very little is known about the role of LSCs in LR (Balabaud et al., 2004). As far as we know, it has been demonstrated through the work of Asahina et al. (2002) that stellate cells could promote hepatocyte regeneration by secreting cytokines after partial hepatectomy (PH). The study conducted by Passino et al. (2007) demonstrated that the neurotrophin signaling pathway in LSCs contributes to hepatocellular growth by stimulating HGF secretion after liver injury. Until now, it has been unclear whether stellate cells are indispensable for promoting hepatocellular regeneration. Therefore, measuring the transcription profiles in stellate cells during the regeneration process would help understand the relevance of this cell population to liver regeneration at the molecular level. Chip assays have been used on stellate cells to yield new insights into its biology (Asselah et al., 2007). However, this technique requires a lot of stellate cells. In the early 1980s, Knook et al. (1982) utilized density gradient centrifugation to isolate stellate cells. However, the stellate cell fraction obtained by this method alone was always contaminated by ~5% of other nonparenchymal cells. In this study, we obtained stellate cells of high purity from rat regenerating liver through a combination of density gradient centrifugation with immunomagnetic bead sorting. The gene expression profiles of LSCs were analyzed during LR using a rat genome 230 2.0 array and the changes in the biological activities predicted by the transcriptome atlas of

[1]College of Life Science, Henan Normal University, Xinxiang 453007, China, [2]Co-constructing Key Laboratory for Cell Differentiation Regulation, Henan Normal University, Xinxiang 453007, China, [3]College of Life Science and Technology, Xinjiang University, Urmuqi 830046, China
*Correspondence: cellkeylab@126.com.

Received April 29, 2010; revised October 3, 2010; accepted October 12, 2010; published online November 26, 2010

Keywords: gene expression profiles, liver regeneration, liver stellate cell, partial hepatectomy, rat

the cells, thus providing the valuable information about the mechanism of LR at the cellular level.

MATERIALS AND METHODS

Preparation of the rat 2/3 hepatectomy model

A total of 114 adult healthy Sprague-Dawley (SD) rats weighing between 190 ± 20 g were used for this experiment. They were obtained from the Experimental Animal Center of Henan Normal University, and were housed in a controlled temperature room (22 ± 1°C) with a 12:12 h light-dark cycle (light form at 8:00 a.m to 20:00 p.m.) and free access to food and water. The animals were randomized into 19 groups (6 rats per group) consisting of nine PH groups, nine sham operation (SO) groups and one control group. A 2/3 hepatectomy operation was carried out by the method of Higgins and Anderson (1931), with surgical removal of the left lateral and median liver lobes. Nine groups of the partially hepatectomized rats were then allowed access to food and water *ad libitum* for 2, 6, 12, 24, 30, 36, 72, 120 and 168 h, respectively. The rats in the SO groups received the same treatment as those in the PH groups, except that liver lobe oblation was not performed. Rats in the control group, that's 0-hour sample of both SO groups and PH groups, underwent perfusion immediately after surgical removal of the left and median lobes. All operations and handling procedures were strictly in accordance with the current Animal Protection Law of China.

Isolation of liver stellate cells

The rats were anesthetized by ether and sterilized with 75% alcohol prior to opening the abdominal cavity. Rats were subjected to ligation of the inferior vena cava (IVC) both below and above the liver, followed by catheterization of the liver portal vein. The liver was perfused via the portal vein with D-Hank's solution at 37°C at a rate of 10-20 ml/min, followed by perfusion with 0.05% collagenase IV at the same rate. Perfused liver samples from six rats per group were cut into pieces and shake-incubated in 15 ml 0.05% IV-type collagenase solution at 37°C for 15 min. The digested sample was filtered through a 200-mesh nylon net. The filtrate was centrifuged at 500 g for 3 min, followed by washing the pellet three times in phosphate buffered saline (PBS) buffer at 4°C. Then, the mixed cell suspension was spread on the surface of a discontinuous Percoll densityt gradient column (4 ml) for centrifugation at 400 × *g* for 5 min at 4°C. The resulting pellet contained LSCs-enriched liver nonparenchymal cells (NPC). The cell density was adjusted to 1×10^8 cells/ml and the cells were mixed with 10 ul/ml of rat GFAP antibody for 15 min at 4°C, then with 10 ul/ml of anti-GFAP-PE for another 15 min, and then the cell suspension was added to 10 ul/ml of rat anti-PE magnetic beads. After loading the cell suspension onto a separation column in a magnetic field, the sample was allowed to flow freely until all the solution had passed through the column. The magnetic field was removed, and the separation column was washed twice in PBS buffer at 4°C. The eluted fractions contained LSCs. The cell survival rate was then evaluated by the trypan blue staining method.

Immunocytochemical analysis

A few purified liver stellate cells were fixed with 10% formaldehyde for 30 min, and then smeared onto glass slides. When the cell suspension had dried on the glass slide, microwave antigen retrieval performance was done. The sections were incubated separately with a 1:200 dilution (V/V) of DES and VIM antibodies overnight at 4°C and then with a 1:5000 (V/V) diluted biotin-labeled secondary antibody at 37°C for 60 min. Streptavidin-biotin complex (SABC) hybridization was then performed at 37°C for 30 min and the sections were observed and analyzed under an optical microscope.

Microarray detection

Total RNA from the isolated LSCs of six rats per group at different time points was pooled using a Trizol mini kit (Invitrogen Corporation, USA) according to the manufacturer's instructions (Norton, 1992), and then quantified by optical density measurement at 260/280 nm and agarose electrophoresis (180 V, 0.5 h) (Scott, 1995). Total RNA from stellate cells at different time points after PH was used for array analysis. Nineteen independent microarray (one genechip corresponds to a cell sample at one time point) analyses were performed using the Affimetrix rat genome 230 2.0 chip (Affymetrix Inc., USA) (Wang et al., 2009). To minimize for technical errors from array analyses, the cell sample in each time point was arrayed repeatedly for three times using the rat genome 230 2.0 array, totaling 3 arrays × 19 groups.

Data analysis and normalization

GCOS 2.0 software (Affymetrix) was used to evaluate the expression signals generated by rat genome 230 2.0 array. The data for each microarray were normalized by scaling all signals to a target intensity of 300. Each probe set used in the Affymetrix GeneChip produces a detection call, with P (present call, requiring a p value < 0.05) indicating good quality, M (marginal call, requiring a 0.05 < p value < 0.065) indicating intermediate quality and A (absent call with a p value > 0.065) indicating relatively low reliability. Therefore, probe sets that resulted in A calls in the compared groups were removed to filter false positives. Next, fold change (the ratio of the normalized signal value of the surgical groups at each time point to that of the control groups) and a T-test performance were applied to select the differentially expressed genes using a fold change threshold of 3.0-fold and a p < 0.05 to indicate significance. e.g., the gene with ⩾ 3-fold higher expression than the control was regarded as up-regulation; the gene with ⩾ 3-fold lower expression than the control, as down-regulation; the gene with 0.33-2.99 fold, as an insignificantly expressed gene. The normalized values of three independent chip analyses at each time point were averaged as the effective values (Guo et al., 2008; Wang et al., 2007).

Quantitative real-time PCR

To verifying the chip data, six genes including *jun, myc, ttr, trim24, des* and *vim* were selected for RT-PCR analysis. Primer sequences for cDNA synthesis were designed by primer express 2.0 software and synthesized by Beijing Sunbiotech Co., Ltd. according to the mRNA sequences of above six genes (Table 1) (Yoon et al., 2002). Before RT performance, Dnase I (Promega) was used to digest the genomic DNA. Total RNA from the isolated LSCs at different time points after PH was individually reverse-transcribed using random primers and a reverse transcription kit (Promega). First-strand cDNA synthesis of the six genes was carried out with SYBR® Green I on Rotor-Gene 3000 (Corbett Robotics). Standard curves were generated from five repeated ten-fold serial dilutions of cDNA, and the copy numbers of target genes in the sample per 1 ml were calculated according to standard curve.

Identification of rat liver regeneration-related genes

Cell samples at each time point were analyzed at least three times using the rat genome 230 2.0 array. One-Way ANOVA

Table 1. Primer sequences of eight genes used to validate microarray results by RT-PCR assay

Symbol	Gene name	Gene ID	Primer sequences (5′ to 3′)	Amplicon length	Tm
Jun	Jun oncogene	NM_021835	FP: TGCAAAGATGGAAACGACCTT RP: GCCGTAGGCGCCACTCT	76 bp	61°C
Myc	Myelocytomatosis viral oncogene homolog	NM_012603	FP: GAGGAGAAACGAGCTGAAGCG RP: TGAACGGACAGGATGTAGGC	126 bp	57°C
Ttr	Transthyretin	NM_012681	FP: ATCGTACTGGAAGGCTCTTGGC RP: CAGTGGTGCTGTAGGAGTAC	131 bp	58°C
Trim24	Tripartite motif-containing 24	AW435169	FP: CAGTGGGAGGGTCTTACAATC RP: CTGGCCAGGGTCTACACTTG	107 bp	58°C
Des	Desmin	NM_022531	FP: CCCTGGCTATTGGCAACTGT RP: CTCGCTGAGGCTTCATTCTG	207 bp	58°C
Vim	Vimentin	NM_031140	FP: CTTGAACGTAAAGTGGAATCCT RP: GTCAGGCTTGGAAACGTCC	135 bp	61°C
Actb	beta-actin	NM_031144	FP: ACATCCgTAAAgACCTCTATgCCAACA RP: GTGCTAGGAGCCAGGGCAGTAATCT	109 bp	62°C

was used to determine the statistical significance of differences between SO groups and PH groups. $P \leq 0.05$ was considered statistically significant and $P \leq 0.01$ was considered very significant. Thus, genes showing a similar expression trend at the same time point in three chip analyses, three-fold or above changes in expression level, and a significant or very significant difference between PH groups and SO groups were defined as liver regeneration-related genes.

H-clustering and principal component analysis

H-clustering and principal component analysis (PCA) approaches are usually performed to analyze the expression data obtained by genechip in an unsupervised manner. H-clustering technique classifies the data by the similarity of gene expression and the results are represented as a dendrogram graph. PCA is used to find the major patterns in data variability. These two methods were used to analyze data obtained from gene chip analysis to group different cell samples into subcategories.

RESULTS

The yield, survival rate and purity of liver stellate cells

Applying the above-described protocol for the isolation of liver stellate cells, we obtained high yields of LSCs (at least 5.84×10^7 cells/rat), as shown in Fig. 1A. Trypan blue staining showed that the cell viability was at least 94% post purification (Fig. 1B). Light microscopy showed that the liver stellate cells had a clear cytoplasm with high refractivity (pictures not shown), and immunocytochemical staining showed that the major portion of the cytoplasm was strongly positive for VIM and DES. It was estimated statistically that the percents of VIM- and DES-positive cells among all the isolated LSCs were at least 95.03% and 95.43%, respectively (Fig. 1C).

Prevalent gene expression patterns of liver stellate cells in liver regeneration

To identify transcriptome changes in LSCs *in vivo* after PH, we measured the gene expression profiles in LSCs using a rat genome 230 2.0 array comprising a total of 24622 probes (corresponding to 24622 genes). After performing the analysis, 10240 genes showed a $\geq$ 3-fold change in expression compared with the control at least at one time point, and had the same or similar expression trend in three array analyses. Taking into consideration the influence of surgical operation on gene expression, we strictly screened the 10240 genes by checking them against the gene expression of cell samples from the SO groups. ANOVA analysis demonstrated that the expressions of 2761 genes had significant or very significant differentiation when compared with the expressions of the SO groups. These 2761 genes were defined as LR-related genes and were clustered into 1113 up-regulated genes, 1336 down-regulated genes and 312 up/down-regulated genes according to their expression patterns.

PCA and hierarchical cluster (H-cluster) analyses were then performed to summarize and visualize the expression patterns of the LR-related genes in LSCs (Fig. 2). PCA analysis of the transcriptional profiles of 2761 genes across all samples demonstrated that the 6 h, 24 h and 30 h samples grouped together; that the 2 h, 12 h and 36 h samples grouped together; and that the 72 h, 120 h and 168 h samples grouped together. The three clusters were distinctly segregated away from each other (Fig. 2A). H-clustering analysis was performed on datasets consisting of the above 2761 genes, resulting in the same results as obtained by PCA (Fig. 2B). Above analyses demonstrated that the samples that clustered together generally had similar biological activities. For instance, the 6-, 30- and 24-hour samples, corresponding to the proliferative phase of LR, clustered together; the 72-, 120- and 168-hour samples, corresponding to the time when the cells were undergoing structural and functional restoration, were classified into one group.

Functional classification of differentially expressed genes

It found that 1563 known genes were included in 2761 LR-related genes, 476 genes of which showed the increased expression, 862 genes the decreased expression and 225 genes the up/down-regulated expression. GO analysis categorized these genes into approximately 25 functional groups. The fraction of genes belonging to each group is shown in Fig. 3. A majority of the up-regulated genes in LSCs encode proteins involved in transport, signal transduction, transcription regulation, cell differentiation and cellular metabolism, occupying 14.07%, 12.18%, 10.29%, 9.87% and 19.29% of the 476 up-

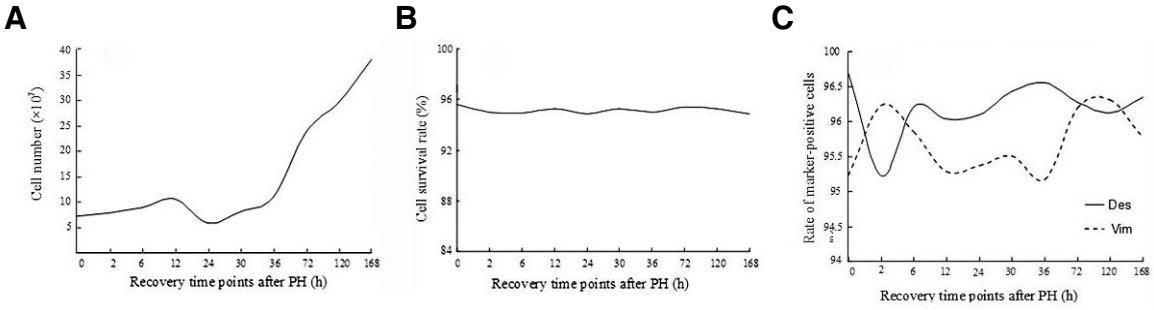

Fig. 1. The yield, survival rate and purity of liver stellate cells. (A) The average number of stellate cell isolated from each rat. (B) The cell survival rate after purification. (C) The percentage of positive LSCs.

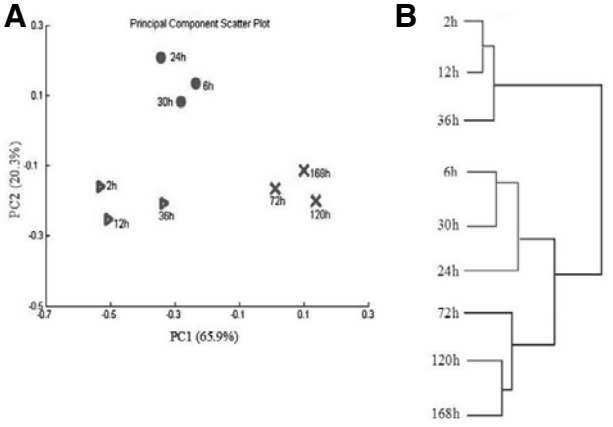

Fig. 2. PCA and H-cluster analysis of microarray data sets from liver stellate cells. (A) PCA analysis of the expression data from 2761 LR-related genes after partial hepatectomy in rats. The first principal component (PC1) is represented by the X-axis, and the second principal component (PC2) is represented by the Y-axis. (B) Enlarged view of the sample dendrogram. H-clustering stratifies the cell samples into two main clusters, the upper branch and basal branch, with the latter further subdivided into two subgroups.

regulated genes in LSCs, respectively. A less pronounced bias was observed for genes responsible for defense responses, stimulus responses, and xenobiotic and macromolecule metabolism, which only represented 1.68%, 1.05%, 1.68% and 1.05% of the up-regulated genes, respectively. Similarly, most of the down-regulated genes in LSCs encode proteins for signal transduction, immunity/inflammation, cell differentiation and transport, accounting for 19.7%, 12.2%, 10.91% and 8.24% of the 862 down-regulated genes, respectively. Notably, the expression of a relatively large proportion of immunity/inflammation-involved genes was significantly reduced in LSCs after PH. While the genes involved in macromolecule, organic acid and xenobiotic metabolism, and cell migration in LSCs only took up a small proportion (in order 0.92%, 0.69%, 0.69%, and 0.81%) of the down-regulated genes. The 225 up/down-expressed genes were categorized into relatively few functional groups. Additionally, there were even fewer genes in amino acid metabolism, apoptosis, cytokine production and organic acid metabolism.

Comparison of gene-expression profiles in different regenerative phases

Usually, the regeneration process is divided into three regenerative phases, including a priming phase (2-6 h post PH), a proliferative phase (6-72 h post PH) and a terminal phase (72-168 h post PH). To explore for differences in biological activities among three regenerative phases, we analyzed the distribution of 476 up-regulated genes and 862 down-regulated genes in the three phases (Fig. 4). The Venn diagram displays the differentially expressed genes detected at different phases of LR in LSCs. The total number of detected genes in each regenerative phase is shown in parenthesis, the number of genes unique to each phase is shown inside the circle, the number of genes detected in two phases is shown in the shaded overlapping areas, and the number of genes detected in all three phases is shown in the central overlap. As shown in Fig. 4, gene expression varied in all three phases, but partially overlapped. To be specific, 77 of 476 up-regulated genes were common to all three phases. These genes were suggestively linked to basic physiological changes in LSC during the entire course of regeneration and coded for proteins involved in transcription regulation (*foxp1*, *hoxc10*, *sox6*, *zfp238 etc*), lipid metabolism (*hsd17b2*, *tdh*, *vldlr etc*), cytokine secretion (*il6*, *p2rx7*, *scg5 etc*) and G-protein-coupled signaling (*gabra5*, *gpr149*, *ltk etc*) (Supplementary Table 3), as shown by gene function analysis. An analysis of the up-regulated genes unique to each phase (Fig. 4A) showed that 50 genes were specifically expressed in the priming phase, 86 genes in the proliferative phase and 4 genes in the terminal phase. A functional analysis of the genes unique to the three phases revealed a prevalence of pathway linked to cellular metabolism rather than to cytokine secretion or immunity/inflammation (Supplementary Tables 1-2; Note, the uniquely expressed genes in terminal phase are not listed). The third set of up-regulated genes corresponded to those that were common to two regenerative phases (for priming and proliferative phases, 242 up-regulated genes were detected; for proliferative and terminal phases, 14 up-regulated genes were detected). Gene function annotation showed that these genes were linked to transport processes (e.g., small molecules, ions) and cellular metabolism (e.g., lipid, protein, xenobiotic substances).

According to Fig. 4B, 61 of 862 down-regulated genes were common to all three phases. These genes were also functionally characterized by GO analysis. The results showed that the great majority of immunity/inflammation involved-genes were markedly down-regulated, while most of the genes involved in transcription regulation, cytokine secretion and signal transduction (Supplementary Table 7) were significantly up-regulated. Analysis of the down-regulated genes unique to each of the three phases revealed that 16 genes down-regulated specifically in the priming phase belong to the categories “cellular metabolism” and “immune/inflammatory response” (Supplementary Table 4); 317 genes unique to the proliferative phase belong to the categories “immunity/inflammation”, “defense

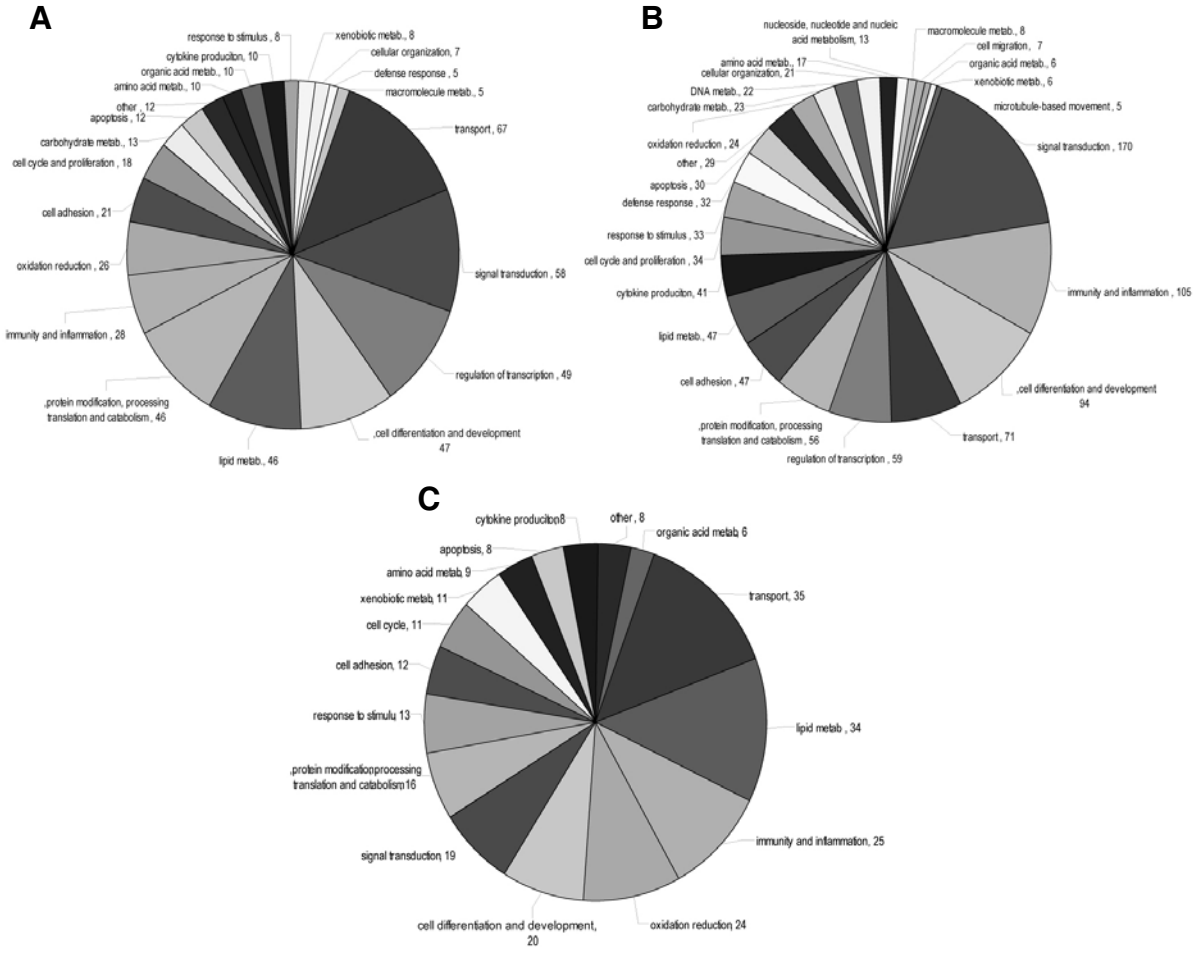

Fig. 3. Functional analysis of the 1563 known genes in LSCs. Pie charts represent the number of genes in each functional group. (A) Functional categories of up-regulated genes. (B) Functional categories of down-regulated genes. (C) Functional categories of up/down-regulated genes.

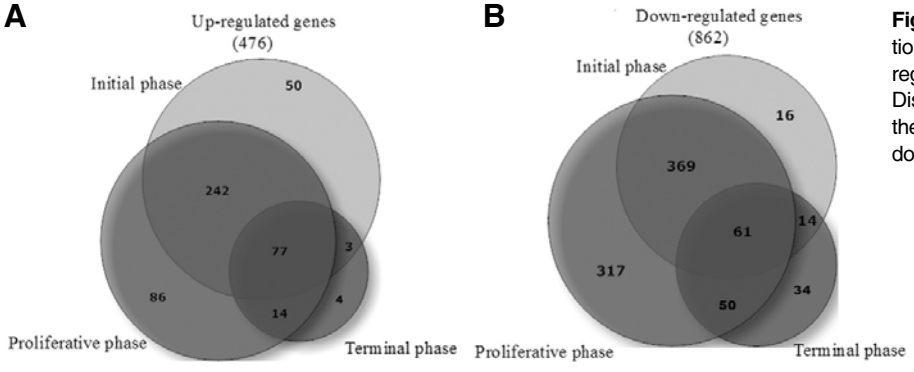

Fig. 4. Venn diagram showing the distribution of the up-regulated and down-regulated genes in three phases of LR. (A) Distribution of the up-regulated genes in the three phases. (B) Distribution of the down-regulated genes in the three phases.

response", "metabolism", "cytokine secretion" and "signal transduction". The category "Signal transduction" was further subcategorized into the signaling pathways mediated by cytokine and chemokine, integrins, T-cell receptor, JNK and NFκB (Supplementary Table 5). Finally, the functional pathway analysis of 34 genes down-regulated specifically in the terminal phase did not reveal any specific biological pathway except cell metabolism (Supplementary Table 6).

Confirmation of chip data by RT-PCR

To evaluate the validity of the chip data obtained in this study, we selected six genes for RT-PCR assays. The genes surveyed were composed of two housekeeping genes *jun* and *myc*, two LSC marker genes *des* and *vim*, and two commonly used genes *ttr* and *trim24*. Total RNA for RT-PCR analysis was extracted from the LSCs at different time points after rat PH. The results showed that, on the whole, the expression levels and trends of the six genes detected by RT-PCR were in ac-

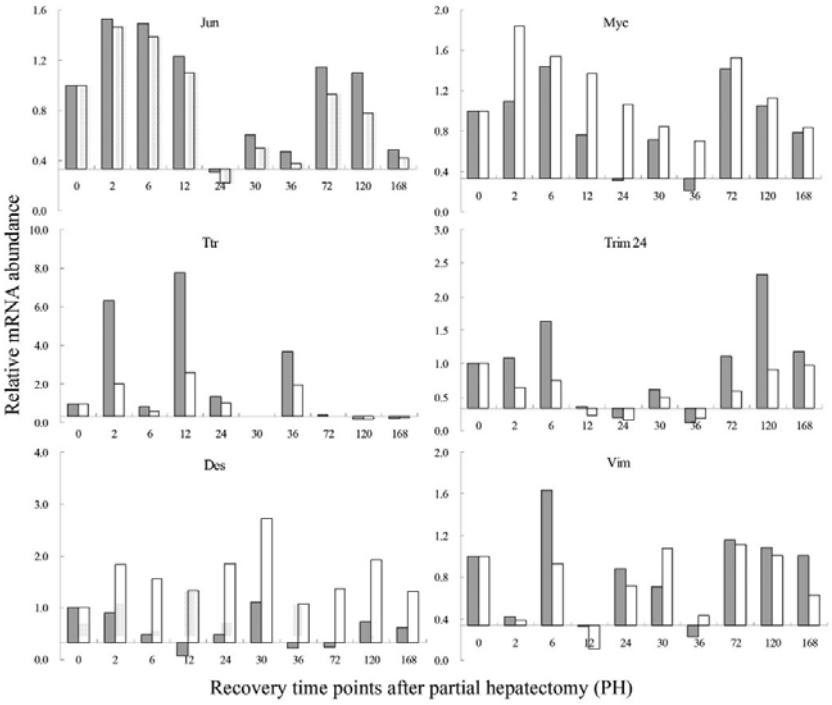

Fig. 5. Verification of gene expression in LSCs by real-time PCR analysis. The results of RT-PCR and rat genome 230 2.0 array analysis are presented as a gray bar and a spotted bar, respectively.

cordance with those obtained by chip analysis, suggesting that array results were reliable (Fig. 5).

DISCUSSION

Although there have been many reports about the biology of LSCs, very little is known about the biological changes occurring in stellate cells during LR at the molecular level (Asselah et al., 2007). Despite the development of new technologies for studying genome-wide gene expression, most of our current knowledge of LSC biology was obtained through conventional methods (Marrack et al., 2000). In this study, we presented a high-throughput strategy for systematically studying the transcriptional profiles in LSCs after PH. First, liver stellate cells with high purity and viability were obtained by using Percoll density gradient centrifugation and immunomagentic bead sorting. The Affymetrix rat genome 230 2.0 array was then used to measure the transcriptional profiles of LSCs after PH in rats.

Our study identified that 1563 known genes were related to LR. According to the expression patterns, 1563 known genes were grouped into three classes: up-regulation, down-regulation (accounting for $\geq$ 55%) and up/down-regulation. When gene functions were taken into consideration, the category "immunity/inflammation" was dominated by down-regulated genes, such as genes encoding chemokines (*ccl2*, *ccr2*, *cxcl2 etc)*, interferons (*ifi35*, *ifi30 etc*), interleukins (*il1a*, *il2b etc*) and complements (*c1qa*, *c1qb etc*), which was inconsistent with the observations of others. For instance, Schwabe et al. (2003) observed that the activated stellate cells highly expressed the proinflammatory factors MCP1, CCL21 and CCR5. It is widely accepted that stellate cells are a major source of cytokines in the liver (Clavien, 2008). Our chip results showed that the mRNA levels of a majority of cytokines and their regulatory genes were significantly decreased in LSCs, which were just the biological characteristics of the inactivated LSCs. Following liver injury caused by PH, liver stellate cells become activated, accompanying with a gradual decrease in retinol levels and the increase in the synthesis of proteins including cytoskeleton components, extracellular matrix proteins, growth factors and cytokines (Schnabl et al., 2002). The present study detected the increased expressions of the retinol production-involved genes *rdh2*, *rdhe2*, and the decreased expressions of retinol esterification-involved gene *lrat* and the retinol export-involved genes *rbp1*, *rbp4* and *rbp7*. These results imply an accumulation of the retinoids in rat liver stellate cells during LR. Based on above analysis, it suggested that the loss of retinoids is not necessarily one of the important features for LSC activation.

In LSCs, the genes up-regulated in all three phases of LR were mainly distributed in the category "lipid metabolism", which could reflect the enhanced lipid metabolism in stellate cells after PH. Meanwhile, there were two groups of up-regulated genes separately unique to the priming phase and proliferative phase. And function analysis of these genes showed that the most populated pathway was metabolic processes including lipid metabolism, indicating perhaps that the biological activities of LSCs post surgery were partly driven by the metabolic pathways. Also, the functional analysis of the up-regulated genes overlapping two phases revealed that they were linked to cell cycle transitions (*acvr1, llgl2 etc*), cell differentiation (h*oxc10*, *glrb etc*), regulation of carbohydrate and lipid metabolisms (*aldh5a1*, *flt3 etc*), and signal transduction via FGF, BMP, integrin and neuropeptide, suggesting the involvement of these genes in transition between the two phases. The above results suggest that lipid metabolism was enhanced in LSCs after PH.

An obvious point to make about the chip data was that the number of down-regulated genes was nearly twice that of up-regulated gene in LSCs. GO analysis demonstrated that the down-regulated genes mainly belonged to the following functional groups: signal transduction, immunity/inflammation, cell differentiation, transport, transcription regulation, and cytokine secretion and its regulation. Notably, a large proportion of the genes involved in immunity/inflammation and cytokine secretion

were down-regulated at least 3-fold after PH, probably predicting the repression of immune response and cytokine secretion in LSCs, which contradicts the findings of recent publications (Xia et al., 2010). As indicated by our results, the down-regulated genes unique to each phase were also involved in immunity/inflammation, which again reinforces the above hypothesis that LSC inactivates cellular immunity and cytokine secretion. However, it is still unclear whether this is due to the weak susceptibility of LSCs to injury stimulus. This should be investigated in a future study. In addition, functional analysis of the down-regulated genes shared by two phases revealed that they were mainly involved in cellular metabolism. Moreover, most of the genes down-regulated in both the priming and proliferative phases were involved in "immunity/inflammation", "defense response" and "immune pathways via B-cell receptor and NFκB", suggesting that LSCs had suppressed immunity/inflammation after PH in rats.

Clearly, there were many differences between our chip data and the published data. Here, we tried to ensure that the transcriptional profiles measured by the gene chip reflected the real changes in the biological activity of the LSCs. First of all, each cell sample was analyzed at least three times with the arrays, thus reducing technical errors from array analysis. Secondly, this study selected 6 representative genes for RT-PCR, and found that their expression profiles were in agreement with those detected by gene chip analysis. Thus, the chip data used in this study is thought to reflect the transcriptional changes of LSCs during LR.

In conclusion, the involvement of a large percentage of down-regulated genes in protein secretion and retinol metabolism suggests that retinoid may be not one of the requirements for LSC activation. By comparing the biological functions of up-regulated genes with those of down-regulated genes, we suggest that lipid metabolism in LSCs was enhanced after PH, while the immune response was not obviously changed. Because of the seemingly contradict results, it is hard to identify the activation state of LSCs during the course of regeneration. This means that it will be difficult to determine the ratio of inactive cells to active cells. Thus, we will further test the above results with other techniques, such as immune staining, in situ hybridization, and fluorescent cell sorting.

Note: Supplementary information is available on the Molecules and Cells website (www.molcells.org).

ACKNOWLEDGMENT

This work was supported by the National Basic Research 973 Pre-research Program of China (No. 2010CB534905)

REFERENCES

Asahina, K., Sato, H., Yamasaki, C., Kataoka, M., Shiokawa, M., Katayama, S., Tateno, C., and Yoshizato, K. (2002). Pleiotrophin/heparin-binding growth-associated molecule as a mitogen of rat hepatocytes and its role in regeneration and development of liver. Am. J. Pathol. *160,* 2191-2205.

Asselah, T., Bieche, I., Paradis, V., Bedossa, P., Vidaud, M., and Marcellin, P. (2007). Genetics, genomics, proteomics: implications for the diagnosis and the treatment of chronic hepatitis C. Semin. Liver Dis. *27*, 13-27.

Atzori, L., Poli, G., and Perra, A. (2009). Hepatic stellate cell: a star cell in the liver. Int. J. Biochem. Cell Biol. *41,* 1639-1642.

Balabaud, C., Bioulac-Sage, P., and Desmoulière, A. (2004). The role of hepatic stellate cells in liver regeneration. J. Hepatol. *40*, 1023-1026.

Budny, T., Palmes, D., Stratmann, U., Minin, E., Herbst, H., and Spiegel, H.U. (2007). Morphologic features in the regenerating liver--a comparative intravital, lightmicroscopical and ultrastructural analysis with focus on hepatic stellate cells. Virchows Arch. *451*, 781-791.

Clavien, P.A. (2008). Liver regeneration: a spotlight on the novel role of platelets and serotonin. Swiss Med. Wkly. *138*, 361-370.

Guo, W., Cai, C., Wang, C., Zhao, L., Wang, L., and Zhang, T. (2008). A preliminary analysis of genome structure and composition in Gossypium hirsutum. BMC Genomics *9*, 314.

Higgins, G.M., and Anderson, R.M. (1931). Experimental pathology of the liver: restoration of the liver of the white rat following partial surgical removal. Arch. Pathol. *12*, 186-202.

Knook, D.L., Seffelaar, A.M., and de Leeuw, A.M. (1982). Fat-storing cells of the rat liver. Their isolation and purification. Exp. Cell Res. *139*, 468-471.

Kubota, H., Yao, H., and Reid, L.M. (2007). Identification and characterization of vitamin-A storing cells in fetal liver: implication of functional importance of hepatic stellate cells in development and hematopoiesis. Stem Cells *25*, 2339-2349.

Marrack, P., Mitchell, T., Hildeman, D., Kedl, R., Teague, T.K., Bender, J., Rees, W., Schaefer, B.C., and Kappler, J. (2000). Genomic-scale analysis of gene expression in resting and activated T cells. Curr. Opin. Immunol. *12*, 206-209.

Mohammed, F.F., and Khokha, R. (2005). Thinking outside the cell: proteases regulate hepatocyte division. Trends Cell Biol. *15*, 555-563.

Norton, J.N. (1992). Total RNA isolation by a rapid centrifugation method. Am. Biotechnol. Lab. *10*, 41.

Passino, M.A., Adams, R.A., Sikorski, S.L., and Akassoglou, K. (2007). Regulation of hepatic stellate cell differentiation by the neurotrophin receptor p75NTR. Science *315*, 1853-1856.

Schnabl, B., Choi, Y.H., Olsen, J.C., Hagedorn, C.H., and Brenner, D.A. (2002). Immortal activated human hepatic stellate cells generated by ectopic telomerase expression. Lab. Invest. *82*, 323-333.

Schwabe, R.F., Bataller, R., and Brenner, D.A. (2003). Human hepatic stellate cells express CCR5 and RANTES to induce proliferation and migration. Am. J. Physiol. Gastrointest. Liver Physiol. *285*, G949-958.

Scott, R.J. (1995). Isolation of whole cell (total) RNA. Methods Mol. Biol. *49*, 197-202

Wang, J.Z., Du, Z., Payattakool, R., Yu, P.S., and Chen, C.F. (2007). A new method to measure the semantic similarity of GO terms. Bioinformatics *23*, 1274-1281.

Wang, W.B., Fan, J.M., Zhang, X.L., Xu, J., and Yao, W. (2009). Serial expression analysis of liver regeneration-related genes in rat regenerating liver. Mol. Biotechnol. *43*, 221-231.

Xia, Y., Chen, R., Song, Z., Ye, S., Sun, R., Xue, Q., and Zhang, Z. (2010). Gene expression profiles during activation of cultured rat hepatic stellate cells by tumoral hepatocytes and fetal bovine serum. J. Cancer Res. Clin. Oncol. *136*, 309-321.

Xiao, P., Tang, A., Yu, Z., Gui, Y., and Cai, Z. (2008). Gene expression profile of 2058 spermatogenesis- related genes in mice. Biol. Pharm. Bull. *31*, 201-206.

Yoon, J.R., Laible, P.D., Gu, M., Scott, H.N., and Collart, F.R. (2002). Express primer tool for high-throughput gene cloning and expression. Biotechniques *33*, 1328-3133.

Zheng, Z.Y., Weng, S.Y., and Yu, Y. (2009). Signal molecule-mediated hepatic cell communication during liver regeneration. World J. Gastroenterol. *15*, 5776-5783.